Cold-target recoil-ion momentum spectroscopy for diagnostics of high harmonics of the extreme-ultraviolet free-electron laser light source at SPring-8

X.-J. Liu,[1,2,b)] H. Fukuzawa,[1,2] G. Prümper,[1,2] M. Okunishi,[1] K. Shimada,[1] K. Ueda,[1,2,a)] K. Motomura,[2,3] N. Saito,[2,3] H. Iwayama,[2,4] K. Nagaya,[2,4] M. Yao,[2,4] A. Rudenko,[2,5] J. Ullrich,[2,5,6] L. Foucar,[2,7] A. Czasch,[7] H. Schmidt-Böcking,[7] R. Dörner,[7] M. Nagasono,[2] A. Higashiya,[2] M. Yabashi,[2] T. Ishikawa,[2] H. Ohashi,[2,8] and H. Kimura[2,8]

[1]*Institute of Multidisciplinary Research for Advanced Materials, Tohoku University, Sendai 980-8577, Japan*
[2]*RIKEN, XFEL Project Head Office, Kouto 1-1-1, Sayo, Hyogo 679-5148, Japan*
[3]*National Metrology Institute of Japan, AIST, Tsukuba 305-8568, Japan*
[4]*Department of Physics, Kyoto University, Kyoto 606-8502, Japan*
[5]*Max Planck Advanced Study Group, CFEL, D-22607, Hamburg, Germany*
[6]*Max Planck-Insitut für Kernphysik, D-69117 Heidelberg, Germany*
[7]*Institut für Kernphysik, Universität Frankfurt, D-60486 Frankfurt, Germany*
[8]*Japan Synchrotron Radiation Research Institute, Kouto 1-1-1, Sayo, Hyogo 679-5198, Japan*

(Received 2 March 2009; accepted 9 April 2009; published online 5 May 2009)

We have developed a cold-target recoil-ion momentum spectroscopy apparatus dedicated to the experiments using the extreme-ultraviolet light pulses at the free-electron laser facility, SPring-8 Compact SASE Source test accelerator, in Japan and used it to measure spatial distributions of fundamental, second, and third harmonics at the end station. © *2009 American Institute of Physics.* [DOI: 10.1063/1.3126422]

I. INTRODUCTION

In October 2007, a new facility, the SPring-8 Compact SASE Source (SCSS) test accelerator in Japan,[1] has started operation. It is the second extreme-ultraviolet (EUV) free-electron laser (FEL) light source in operation after the one at Hamburg (FLASH).[2] The SCSS test accelerator provides linearly polarized EUV-FEL (~30 μJ per pulse, ~100 fs pulse width, and 10–20 Hz repetition rate) in the wavelength region 51–61 nm under laser power saturation conditions. This energy regime is of particular interest because all atoms, except helium, in any forms of matter, can be ionized with huge photoionization cross sections. This new source, however, requires redesigning the experimental end stations and the particle detection systems compared to those used at synchrotron sources or optical laser sources with high repetition rates $\geq$1 kHz. For the EUV-FEL concerned, even under ultrahigh vacuum conditions of 10^{-10} Torr, the unfocused FEL beam produces hundreds of electrons and ions from residual gas per laser shot. Furthermore, if any tiny fraction of the scattered light from the surface of mirrors and slits hit a metal surface of the electron spectrometer, thousands of electrons are produced, making momentum or velocity imaging very difficult.

To circumvent difficulties described above, we have developed a dedicated apparatus for cold-target recoil-ion momentum spectroscopy (COLTRIMS) (Ref. 3) and employed it to characterize the higher order harmonics of the FEL beam. For studies of two- and three-photon processes in the FEL focus, it is nontrivial to distinguish these processes from single-photon processes of the second and third harmonics of the FEL and hence a careful characterization of the FEL beam is essential. The next section describes the design of the apparatus. In Sec. III, we describe the experimental procedure for the measurements of spacial distributions for the fundamental, second, and third harmonics of the FEL beam. Section IV illustrates the experimental results, whereas Sec. V is a brief summary.

II. DESIGN OF THE APPARATUS

The design of our ion spectrometer, shown in Fig. 1, is similar to the one described in Ref. 4. The spectrometer uses two acceleration regions with homogenous electric fields and a drift tube. The source volume of the ions is the intersection of the gas beam and the FEL beam. It is 30 mm away from the extractor electrode and 25.1 mm away from the pusher electrode. The pusher and extractor electrodes are plane aluminum plates with round holes covered by flat stainless steel meshes (70% transmission each). The second acceleration region is 61.6 mm long. After the second acceleration region the extracted ions enter the 268 mm long drift tube. It is terminated by two grids to obtain a field free region inside. With three meshes of 70% transmission each and the detector of 30% detection efficiency, the overall detection efficiency is about 10%. The voltages of the electrodes are usually set to values that fulfill the space focusing condition. Relatively high mass resolution (>100) is achieved to resolve the signals by target from those by residual gases.

The determination of the ion momentum is based on the measurements of the time-of-flight (TOF) and the detector

[b)]Electronic mail: xjliuxjliu@gmail.com.
[a)]Electronic mail: ueda@tagen.tohoku.ac.jp.

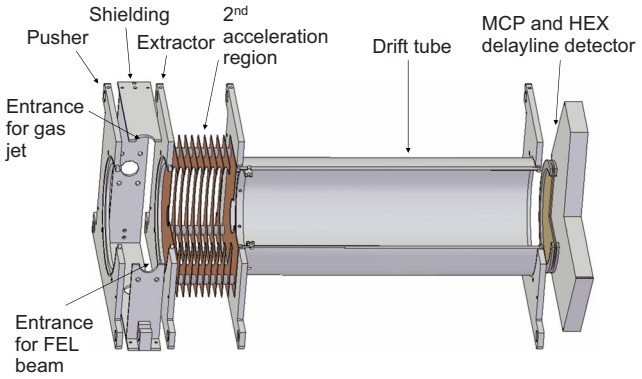

FIG. 1. (Color online) Cut through the ion momentum spectrometer.

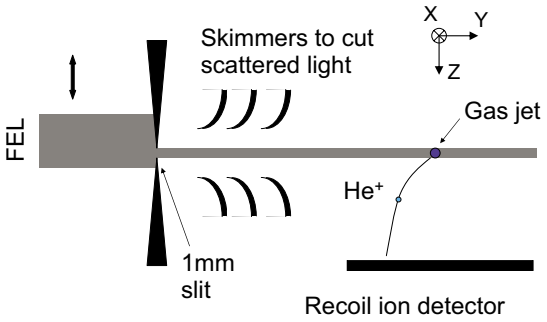

FIG. 2. (Color online) Experimental alignment.

hit position for each ion.[3,5] Here, a three-layer delay-line anode (Roentdek HEX80) was used for the readout of the microchannel plate (MCP) in order to minimize the dead-time.[6] A combination of obtaining redundant information from the three layers of the delay-line anode and a sophisticated logic is necessary to reconstruct time and positions of all "hits." Instead of conventional constant fraction discriminators and time-to-digital converters, an 8-channel digitizer (Acqiris DC282×2) was used.[7,8] The complete waveforms of six signals from the three-layer delay-line anode and one from the MCP were recorded by seven channels of the 8-channel digitizer and stored in the computer. The timing signals were extracted off line from each waveform by a software simulating a constant fraction discriminator.[9] In this way we could separate up to eight detected ions within 100 ns. More than 100 ions can be recorded per laser shot in the TOF of 20 μs.

The target beam is produced by expanding the sample gas with a stagnation pressure from 1 to 10 atm through a nozzle with a pinhole of 30 μm in diameter and 250 μm in thickness. The nozzle can be cooled and temperature stabilized between room temperature and 130 K. The supersonic beam is skimmed by a 0.5 mm diameter 30° skimmer about 10 mm in front of the nozzle. The nozzle is housed in a CF150 cross. For differential pumping, two apertures, with diameters of 1 mm, are mounted at 400 and 610 mm downstream. The main vacuum chamber follows the second differential pumping stage. On the other side of the main chamber, a beam dump is mounted consisting of a 10 mm hole. Under typical operating conditions using a stagnation pressure of 3 atm in the nozzle, the pressures in the source chamber, the first differential pumping stage, the main chamber, and the beam dump are 2.6×10^{-4}, 3.1×10^{-8}, 1.3×10^{-10}, and 8.0×10^{-10} torr, respectively. The pressure read in the main chamber does not depend on the presence of the target gas beam. The beam propagation direction is vertical from top to bottom.

III. EXPERIMENT

We have used this new apparatus to characterize the higher order harmonics of the EUV-FEL provided by the SCSS test accelerator. The experimental alignment is shown in Fig. 2. A cooled (130 K) supersonic jet of helium was used as a target. The unfocused FEL beam passes through the spectrometer horizontally steered by one of the two upstream SiC plane mirrors. At ~1 m in front of the spectrometer, the unfocused FEL beam is cut by a slit with 1 mm opening. Three skimmers are installed to suppress the scattered light from the edge of the slit. The field strength and the ponderomotive energy of the unfocused FEL beam are about 2×10^{8} W/cm^2 and 6×10^{-8} eV, respectively. The Keldysh parameter for the ionization of helium is about 1.4×10^{4}. Thus all the multiphoton processes can be neglected and all electrons emitted from helium atoms with high kinetic energies are due to ionization by the higher harmonics only. For single ionization the momentum vectors of the photoelectron and of the ion are almost equal and opposite. The photon momentum is negligible at these energies. Technically, however, it is easier to measure the recoil momenta of the helium ions than to measure the electron kinetic energy, because the electrons emitted from the residual gas completely mask the electrons from the helium target. The TOF spectrometer axis is parallel to the electric vector of the FEL beam. The electrostatic fields 0.24 and 0.93 V/mm in the two acceleration stages, respectively, project He^+ ions with kinetic energies up to 90 meV onto a 80 mm diameter MCP in front of the delay-line anode, so that we can clearly resolve the recoil of the He^+ ion charge state and momentum vector in the TOF and the detector hit position. The count rate in the He^+ ion signal was less than one count per laser shot, far less than about 40 ions detected per laser shot, originating from the residual gas at 10^{-10} Torr. It took about 45 min to record data at one position at the FEL repetition rate of 10 Hz. In total, about 6 h were spent on the data acquisition for all the positions scanned.

The spectral distributions of FEL pulses recorded by the EUV spectrometer equipped with the optical multichannel analyzer just before the present measurement is shown in Fig. 3. The distribution varies shot by shot as nature of SASE. After averaging many shorts, we find that, for the used settings of the FEL, about 0.1% of the spectrum has a wavelength shorter than 50.42 nm, corresponding to the ionization energy of He of 24.59 eV. Accordingly, only this small fraction of the fundamental radiation, besides the higher harmonics, contributes to the ionization of helium. It should be noted that the EUV spectrometer is optimized to measure FEL spectrum around 50–60 nm, and the shortest wavelength limit is about 30 nm. It is difficult to quantitatively determine the contribution of higher order light using the EUV spectrometer.

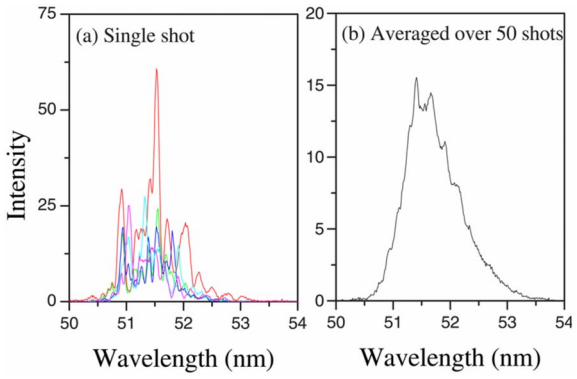

FIG. 3. (Color online) Spectral distribution of EUV-FEL pulses. (a) Five spectra for individual FEL shots and (b) average of over 50 laser shots.

IV. RESULTS AND DISCUSSION

The momentum resolution is the best along the polarization direction that coincides the with TOF spectrometer axis (Z) and the direction of the FEL beam propagation (X). These two directions are both perpendicular to the gas jet, as the transversal spread of the momenta in the jet are very small due to skimming of the target. The two-dimensional (2D) plots, P_x versus P_z, of He^+ ion momentum distributions are shown in Fig. 4. The spectrum was recorded with the central portion of the FEL beam. We can clearly identify the He^+ momentum distributions for single-photon ionization by the second and third harmonics. Their angular distributions are well described by the $\cos^2\theta$ distributions of the p wave, with θ being the angle between the polarization direction and the recoil-ion momentum. This also confirms that these momentum distributions are not due to the two- and three-photon ionizations by the fundamental that produces high-l waves. The resolution in the third Cartesian coordinate is not sufficient to clearly resolve the different orders of the FEL beam. We used this coordinate only to discriminate against ion signals coming from residual helium gas in the vacuum chamber by restricting the analysis to an appropriate Y interval on the detector.

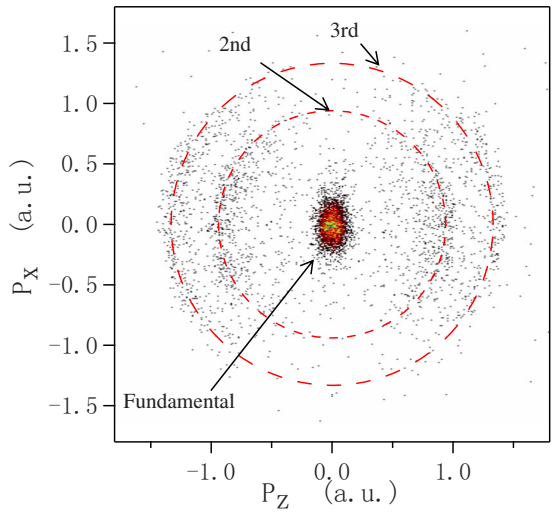

FIG. 4. (Color online) 2D recoil momentum distribution of He^+. The dashed circles indicate the momentum positions for single-photon ionization of the second and third harmonics. The spectrum was recorded with the central potion of the FEL beam.

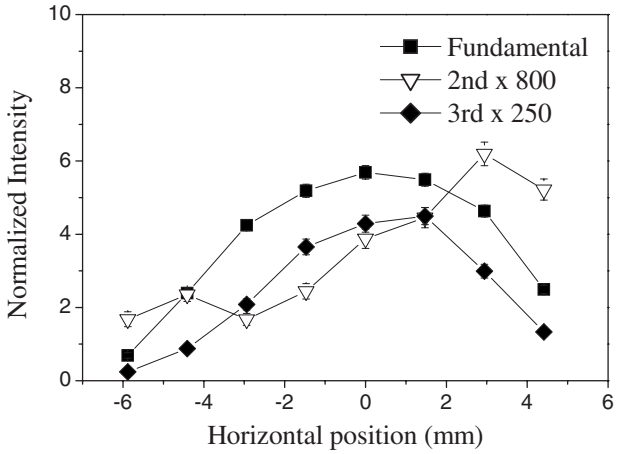

FIG. 5. Spatial distributions of the intensity for the fundamental, the second, and the third harmonics in the experimental chamber.

The data were accumulated and analyzed for each setting of the steering mirror that changes the position of the unfocused FEL beam. In this way a profile of the contributions of the fundamental, the second, and the third harmonics were measured as a function of the horizontal position. The results are shown in Fig. 5. Here, we have obtained the relative intensities of the harmonics using known photoionization cross sections of helium atoms at three-photon energies concerned.[10] For the fundamental and the third harmonics, the maximum of the intensity is in the center and the intensities decrease symmetrically. For the second harmonic the intensity is not maximal at the center. Also, the second harmonic has a broader profile than the fundamental and the third harmonics.

The information about the spatial distribution of each harmonic, as well as their relative intensities, are important in distinguishing the two- and three-photon processes from single-photon absorption by the second and third order harmonics. To identify two-photon processes, one usually measures the yields as a function of the photon flux and fits a power law. Our result shows that, by opening the slit, one increases the relative contribution of second harmonics with respect to the fundamental. One has to keep this in mind whenever he tries to measure the two-photon processes.

In principle, the same information could be obtained from conventional electron spectroscopy for the He target. However, performing the electron spectroscopy on the EUV-FEL beam line is by any means nontrivial, due to huge background electron signals from the residual gas and surface emission by the scattered light. In fact, we tried to perform also the electron spectroscopy but the background signals completely masked the very weak signals from the target. The He COLTRIMS measurements employed here were, on the other hand, completely free from such background signals.

V. CONCLUDING REMARK

We constructed a COLTRIMS setup at the SCSS test accelerator beamline at Japan and employed it to measure the

spatial distributions of fundamental, second, and third harmonics from the unfocused FEL beam. We found that their relative contributions change as a function of the horizontal positions in the FEL beam. This measurement was possible because the COLTRIMS was free from the background that made electron spectroscopy extremely difficult or practically impossible.

ACKNOWLEDGMENTS

We are grateful to Takashi Tanaka for very helpful discussion about the high harmonics of the FEL beam, to the SCSS Test Accelerator Operation Group at RIKEN for continuous support in the course of the studies, and to the staff of the technical service section in IMRAM, Tohoku University, for their assistance in constructing the apparatus. This study was supported by the XFEL Utilization Research Project of the Ministry of Ecucation, Science, and Technology (MEST), by JSPS, by the IMRAM, by the MPG Advanced Study Group within CFEL, and by BMBF.

[1] T. Shintake, H. Tanaka, T. Hara, T. Tanaka, K. Togawa, M. Yabashi, Y. Otake, Y. Asano, T. Bizen, T. Fukui, S. Goto, A. Higashiya, T. Hirono, N. Hosoda, T. Inagaki, S. Inoue, M. Ishii, Y. Kim, H. Kimura, M. Kitamura, T. Kobayashi, H. Maesaka, T. Masuda, S. Matsui, T. Matsushita, X. Marechal, M. Nagasono, H. Ohashi, T. Ohata, T. Ohshima, K. Onoe, K. Shirasawa, T. Takagi, S. Takahashi, M. Takeuchi, K. Tamasaku, R. Tanaka, Y. Tanaka, T. Tanikawa, T. Togashi, S. Wu, A. Yamashita, K. Yanagida, C. Zhang, H. Kitamura, and T. Ishikawa, Nat. Photonics **2**, 555 (2008).

[2] V. Ayvazyan, N. Baboi, J. Bähr, V. Balandin, B. Beutner, A. Brandt, I. Bohnet, A. Bolzmann, R. Brinkmann, O. I. Brovko, J. P. Carneiro, S. Casalbuoni, M. Castellano, P. Castro, L. Catani, E. Chiadroni, S. Choroba, A. Cianchi, H. Delsim-Hashemi, G. Di Pirro, M. Dohlus, S. Düsterer, H. T. Edwards, B. Faatz, A. A. Fateev, J. Feldhaus, K. Flöttmann, J. Frisch, L. Fröhlich, T. Garvey, U. Gensch, N. Golubeva, H.-J. Grabosch, B. Grigoryan, O. Grimm, U. Hahn, J. H. Han, M. V. Hartrott, K. Honkavaara, M. Hüning, R. Ischebeck, E. Jaeschke, M. Jablonka, R. Kammering, V. Katalev,B. Keitel, S. Khodyachykh, Y. Kim, V. Kocharyan, M. Körfer, M. Kollewe, D. Kostin, D. Krämer, M. Krassilnikov, G. Kube, L. Lilje, T. Limberg, D. Lipka, F. Löhl, M. Luong, C. Magne, J. Menzel, P. Michelato, V. Miltchev, M. Minty, W. D. Möller, L. Monaco, W. Müller, M. Nagl, O. Napoly, P. Nicolosi, D. Nölle, T. Nuñez, A. Oppelt, C. Pagani, R. Paparella, B. Petersen, B. Petrosyan, J. Pflüger, P. Piot, E. Plönjes, L. Poletto, D. Proch, D. Pugachov, K. Rehlich, D. Richter, S. Riemann, M. Ross, J. Rossbach, M. Sachwitz, E. L. Saladin, W. Sandner, H. Schlarb, B. Schmidt, M. Schmitz, P. Schmüser, J. R. Schneider, E. A. Schneidmiller, H.-J. Schreiber, S. Schreiber, A. V. Shabunov, D. Sertore, S. Setzer, S. Simrock, E. Sombrowski, L. Staykov, B. Steffen, F. Stephan, F. Stulle, K. P. Sytchev, H. Thom, K. Tiedtke, M. Tischer, R. Treusch, D. Trines, I. Tsakov, A. Vardanyan, R. Wanzenberg, T. Weiland, H. Weise, M. Wendt, I. Will, A. Winter, K. Wittenburg, M. V. Yurkov, I. Zagorodnov, P. Zambolin, and K. Zapfe, Eur. Phys. J. D **37**, 297 (2006).

[3] J. Ullrich, R. Moshammer, A. Dorn, R. Dörner, L. Ph. H. Schmidt, and H. Schmidt-Böcking, Rep. Prog. Phys. **66**, 1463 (2003).

[4] G. Prümper, H. Fukuzawa, T. Lischke, and K. Ueda, Rev. Sci. Instrum. **78**, 083104 (2007).

[5] K. Ueda and J. H. D. Eland, J. Phys. B **38**, S839 (2005).

[6] O. Jagutzki, A. Cerezo, A. Czasch, R. Dörner, M. Hattaß, M. Huang, V. Mergel, U. Spillmann, K. Ullmann-Pfleger, T. Weber, H. Schmidt-Böcking, and G. D. W. Smith, IEEE Trans. Nucl. Sci. **49**, 2477 (2002).

[7] A. Czasch, L. Ph. H. Schmidt, T. Jahnke, Th. Weber, O. Jagutzki, S. Schössler, M. S. Schöffler, R. Dörner, and H. Schmidt-Böcking, Phys. Lett. A **347**, 95 (2005).

[8] G. Da Costa, F. Vurpillot, A. Bostel, M. Bouet, and B. Deconihout, Rev. Sci. Instrum. **76**, 013304 (2005).

[9] L. Foucar, Ph.D. thesis, J. W. Geothe University, 2008.

[10] W. F. Chan, G. Cooper, and C. E. Brion, Phys. Rev. A **44**, 186 (1991).